Journal of Pharmaceutical Analysis 9 (2019) 312–323

Contents lists available at ScienceDirect

Journal of Pharmaceutical Analysis

journal homepage: www.elsevier.com/locate/jpa

Original Article

Elucidating the interaction of kansui and licorice by comparative plasma/tissue metabolomics and a heatmap with relative fold change

Yan-Yan Chen [a, 1], Juan Shen [b, 1], Yu-Ping Tang [a, b, *], Jin-Gao Yu [a], Jing Wang [a], Shi-Jun Yue [a], Jie Yang [a], Jia-Qian Chen [b], Li-Mei Feng [a], Zhen-Hua Zhu [b], Wei-Wei Tao [b], Li Zhang [b], Jin-Ao Duan [b, **]

[a] Key Laboratory of Shaanxi Administration of Traditional Chinese Medicine for TCM Compatibility, State Key Laboratory of Research & Development of Characteristic Qin Medicine Resources (Cultivation), Shaanxi Key Laboratory of Chinese Medicine Fundamentals and New Drugs Research, and Shaanxi Collaborative Innovation Center of Chinese Medicinal Resources Industrialization, Shaanxi University of Chinese Medicine, Xi'an 712046, Shaanxi Province, China

[b] Jiangsu Collaborative Innovation Center of Chinese Medicinal Resources Industrialization, National and Local Collaborative Engineering Center of Chinese Medicinal Resources Industrialization and Formulae Innovative Medicine, and Jiangsu Key Laboratory for High Technology Research of TCM Formulae, Nanjing University of Chinese Medicine, Nanjing 210023, Jiangsu Province, China

ARTICLE INFO

Article history:
Received 30 January 2019
Received in revised form
13 April 2019
Accepted 29 May 2019
Available online 1 June 2019

Keywords:
Comparative metabolomics
Kansui
Licorice
Incompatibility
Heatmap

ABSTRACT

Although compatibility is highly advocated in traditional Chinese medicine (TCM), inappropriate combination of some herbs may reduce the therapeutic action and even produce toxic effects. Kansui and licorice, one of TCM "*Eighteen Incompatible Medicaments*", are the most representative cases of improper herbal combination, which may still be applied simultaneously under given conditions. However, the potential mechanism of their compatibility and incompatibility is unclear. In the present study, two different ratios of kansui and licorice, representing their compatibility and incompatibility respectively, were designed to elucidate their interaction by comparative plasma/tissue metabolomics and a heatmap with relative fold change. As a result, glycocholic acid, prostaglandin F2a, dihydroceramide and sphinganine were screened out as the principal alternative biomarkers of compatibility group; sphinganine, dihydroceramide, arachidonic acid, leukotriene B4, acetoacetic acid and linoleic acid were those of incompatibility group. Based on the values of biomarkers in each tissue, the liver was identified as the compatible target organ, while the heart, liver, and kidney were the incompatible target organs. Furthermore, important pathways for compatibility and incompatibility were also constructed. These results help us to better understand and utilize the two herbs, and the study was the first to reveal some innate characters of herbs related to TCM "*Eighteen Incompatible Medicaments*".

1. Introduction

Traditional Chinese medicine (TCM) has gained growing popularity and wide usage in the world in the past several decades. However, the modernization of TCM is still facing many obstacles due to its unimaginable complexity. Herb compatibility, as the basic characteristic of TCM, is of great importance in the study of TCM modernization. In TCM theory, compatibility refers to the combination of two or more herbs based on the clinical settings and the properties of them, which help enhance the therapeutic effects and counteract the toxicities or side effects. Long-term applications have demonstrated that herb compatibility is not only a better choice, but also a necessary one. However, although compatibility is highly advocated in TCM, it does not mean that the combination of

Peer review under responsibility of Xi'an Jiaotong University.

* Corresponding author at: the Key Laboratory of Shaanxi Administration of Traditional Chinese Medicine for TCM Compatibility, State Key Laboratory of Research & Development of Characteristic Qin Medicine Resources (Cultivation), Shaanxi Key Laboratory of Chinese Medicine Fundamentals and New Drugs Research, and Shaanxi Collaborative Innovation Center of Chinese Medicinal Resources Industrialization, Shaanxi University of Chinese Medicine, Xi'an 712046, Shaanxi Province, China.

** Corresponding author.

E-mail addresses: yupingtang@sntcm.edu.cn (Y.-P. Tang), dja@njucm.edu.cn (J.-A. Duan).

[1] These two authors contributed equally to this work.

https://doi.org/10.1016/j.jpha.2019.05.005

herbs always brings benefits. Inappropriate combination of two herbs, for example, may reduce or restrict the therapeutic action of the other, and even produce toxic effects. The phenomenon was early noticed and described as incompatibility. TCM "*Eighteen Incompatible Medicaments*", the most representative cases of improper herbal combination, have been summarized based on the long-term experiences of TCM physicians since the *Jin* and *Yuan* dynasties [1,2], and were strictly observed in ancient and modern clinical medication.

The compatibility of kansui and licorice is a classical representative of TCM "*Eighteen Incompatible Medicaments*". Kansui, the dried roots of *Euphorbia kansui* T. N. Liou ex T. P. Wang and a well-known TCM recorded in Shen Nong's Herbal Classic, has been widely used for centuries in China as a remedy for edema, ascites, and asthma [3]. Recent studies have demonstrated that kansui also has a variety of pharmacological actions including anti-fertility, anti-tumor and immune-regulation [4–6]. Licorice, the dried roots and rhizomas of *Glycyrrhiza uralensis* Fisch., *Glycyrrhiza inflata* Bat., or *Glycyrrhiza glabra* L., is a widely distributed herbal medicine in southern Europe and parts of Asia. Licorice is described in many TCM formulae for its medical activities, such as anti-inflammatory, anti-allergic, antimicrobial, and immune-regulatory effects [7,8]. As a unique "guide drug" in TCM, licorice is commonly combined with other herbs to play the toxicity-reducing and effect-enhancing role in almost half of the Chinese herbal formulae [9,10]. Taking kansui and licorice as an example, the herbal pair has been prescribed in a classical TCM formula (*Gansui Banxia Tang*) for the treatment of cancerous ascites since the *Han* Dynasty, and it was effective for cirrhosis ascites cases in recent clinical trial [11]. However, in many TCM monographs, the compatibility of kansui and licorice was recorded as one of "*Eighteen Incompatible Medicaments*", which was traditionally believed to be antagonistic and thus theoretically should not be applied simultaneously [12]. Additionally, it was found that the combined use of licorice and kansui has a significant impact on cardiac, hepatic and renal functions [13], and the purgative effect of kansui is markedly weakened when combined with licorice [14], which suggests that the two herbs may exhibit synergistic or antagonistic effects in different combination conditions.

Recently, our research group investigated the dosage-toxicity-efficacy relationship of kansui and licorice in malignant pleural effusion (MPE) models [15,16]. The results showed that kansui had certain efficacy for treating MPE, but the efficacy was influenced by co-using with licorice, and even serious toxicity was caused at a given ration. The ratio between 2:1 and 1:1 (kansui: licorice) was considered as the flex point of the dosage-toxicity-efficacy. When the ratio of kansui and licorice was lower than this point, there was a potential therapeutic effect on MPE with negligible toxicity. By contrast, when the ratio was above the flex point, liver, kidney and heart toxicity with unfavorable therapeutic effects occurred. It showed that the compatibility and incompatibility of kansui and licorice were changed with the different ratios and dosages. However, the potential mechanism of this interesting phenomenon is unclear.

Metabolomics, a top-down platform in the field of systems biology, focuses on the dynamic changes of small molecules in response to the disturbance of the organism [17]. Nontargeted metabolomics enables the levels of a broad range of metabolites in parallel assessment and are being widely used for discovering new biomarkers, diagnosing diseases, measuring the response to treatment and identifying perturbed pathways due to disease or toxicity [18,19]. Biofluids such as plasma and urine are commonly considered to be a pool of metabolites that reflect systemic metabolic deregulation, and the markers in these biofluids could reflect the characteristics of the system in diseases state. Evaluation of tissue metabolites is also of great value in metabolomics study which can provide more direct information of metabolism compared with biofluids [20,21].

In this study, two different ratios of kansui and licorice (4:1 and 1:4), which represent their compatibility and incompatibility respectively, were designed to investigate the effect of individual and combined use of kansui and licorice on MPE rats. Furthermore, the comparative metabolomics was employed to explore their mechanisms. Therefore, ultra-performance liquid chromatography with tandem quadrupole time-of-flight mass spectrometry (UPLC-Q/TOF-MS) was used to analyze the metabolic changes in plasma, heart, liver, and kidney of MPE rats; then the multivariate statistical method was utilized for the metabolomic analysis; metabolic pathways were constructed, which was aimed to elucidate possible interaction mechanism for the compatibility and incompatibility of kansui and licorice.

2. Materials and methods

2.1. Herbs and animals

Kansui was the dried roots of *Euphorbia kansui* T.N. Liou ex T.P. Wang, and licorice was the dried roots and rhizomes of *Glycyrrhiza uralensis* Fisch. The extraction and preparation of drug solution were the same as those in our previous study [15]. Fifty-six rats were randomly divided equally into seven groups: normal control group, model group, kansui group, licorice 1 group, licorice 2 group, kansui:licorice 4:1 group, and kansui:licorice 1:4 group. The ratios and doses are listed in Table 1. Detailed description about materials, animals and treatment, sample collection and preparation is provided in Supplemental Data S1.

2.2. Metabolomics study

Metabolomic study was performed on an UPLC-Q-TOF/MS system. UPLC separation was achieved on a Thermo Syncronic C_{18} column (2.1 mm × 100 mm, 1.7 μm) on an Acquity UPLC system (Waters, Millford, USA), whereas mass spectrometry was performed on a Synapt™ quadrupole time of flight mass system (Waters, Millford, USA). Raw UPLC-Q-TOF/MS data acquired were imported to MassLynx software (Version 4.1, Waters, Milford, USA). Data treatment procedures, such as peak alignment, discrimination, filtering, and matching were performed, and the resultant data matrices were imported to EZinfo 2.0 software for principal component analysis (PCA), partial least squares discriminant analysis (PLS-DA) and orthogonal partial least squared discriminant analysis (OPLS-DA). The variables with VIP >1 would be responsible for the separation of samples. The relative distances between treated groups and the control group from PLS-DA score plots were calculated with the average value of all samples of the control group as the referenced point.

Potential biomarkers were extracted from S-plots constructed following analysis with OPLS-DA, and VIP was also used for the selection [22]. Metabolites identification was based on retention time, precise molecular mass, MS/MS data, and online database. The precise molecular mass was determined within a reasonable degree of measurement error (<5 ppm) using Q-TOF, and the potential element composition, degree of unsaturation and fractional isotope abundance of the compounds were also obtained. The MassFragment application manager (MassLynx, Version 4.1) was used to facilitate the MS/MS fragment ion analysis process by way of chemically intelligent peak-matching algorithms. The presumed molecular formula was searched in HMDB, Metlin, and KEGG to identify the possible chemical constitutions, and the MS/MS data were screened to determine the potential structures of the ions. Finally, the metabolites were identified by comparison with the MS/

Table 1
The doses and ratios of different groups.

Groups	Kansui (g/kg)	Licorice (g/kg)	Ratio (kansui:licorice)
Control	–	–	–
Model	–	–	–
Kansui	0.15	–	–
Licorice 1	–	0.04	–
Licorice 2	–	0.60	–
Kansui:licorice 4:1	0.15	0.04	4:1
Kansui:licorice 1:4	0.15	0.60	1:4

MS spectrum in online databases and literature. Pathway analysis was performed with MetaboAnalyst, which is a web-based tool for visualization of metabolomics [23,24].

2.3. Statistical analysis

A novel heatmap with relative fold changes was used to investigate the variations of metabolites visually in herb-combination group. First, differential metabolites between the control group and treated groups were screened out. Then, based on fold changes (FC) of these differential metabolites, the original metabolic heatmap was performed to visualize the degree of metabolites, which could clearly show the biomarker changes in single herb group of kansui or licorice. FC of each metabolite was calculated using the following formulas: if $V_A > V_B$, $FC = V_A/V_B$, if $V_A < V_B$, $FC = -V_B/V_A$, where V_A represents the value of one metabolite in one group, and V_B represents the value of this metabolite in another group. However, the compatibility and incompatibility biomarkers filtered from the herb-combination group were misleading by neglecting herb-herb interaction. Thus, an interactive heatmap with relative fold changes (RFC) was created, which means FC of one metabolite in herb-combination group minus that of in single herb group. RFC of each metabolite in kansui-licorice combination group was calculated using the following formula: $RFC = FC_C - FC_L - FC_K$, where FC_C represents the fold change of one metabolite in kansui-licorice combination group/model group, FC_L represents that in licorice group/model group, and FC_K represents that in kansui group/model group. Finally, a heatmap was used to visualize the change trends of metabolites in each group.

3. Results

3.1. General status, biochemical and histopathological observations

There were noticeable differences in the general status among the different groups. The model group exhibited signs of weight loss and appetite decrease, while these symptoms could be improved by the administration of kansui and kansui: licorice 4:1. The pleural fluid volume of the control, model, kansui, licorice 1, licorice 2, kansui: licorice 4:1 and 1:4 groups was 0.8 ± 0.3, 13.1 ± 2.3, 5.4 ± 1.2, 10.8 ± 1.7, 11.3 ± 2.4, 4.6 ± 1.5, and 12.9 ± 2.1 mL, respectively. The results indicated that kansui and kansui: licorice 4:1 had a certain therapeutic effect on MPE.

Biochemical parameters of different groups are shown in Table 2. Compared with the control group, levels of ALT, BUN, CREA and CK were significantly increased ($P < 0.05$) in the model group, which indicated that the rats in the model group might suffer liver, kidney and heart injuries. The decreased levels of ALT, BUN, CREA and CK in both kansui group and kansui:licorice 4:1 group reflected the therapeutic effect on MPE rats.

Histopathology of heart, liver, and kidney tissues of each group was examined to further investigate the effect or toxicity. As demonstrated in Fig. 1, the heart, liver, and kidney of the control group showed no signs of obvious abnormality or tissue damage, but pathological changes could be observed in the model group. After oral administration of kansui, licorice and their combination, the pathological changes in the liver and kidney were attenuated in kansui: licorice 4:1 group, while heart, liver, and kidney injuries were even worse in kansui: licorice 1:4 group.

3.2. Metabolic profiling of plasma samples

Global metabolic profiling in both positive and negative ion modes was analyzed by UPLC-Q-TOF/MS. The PCA score plot (Fig. 2A) could divide the plasma samples of the control group and the model group into different blocks, suggesting that the metabolic profiles have changed as the result of MPE modeling. The significant differences of endogenous metabolites between the control group and the model group could be found from the S-plots (Fig. 2B). The mass spectrometry signals responsible for this differentiation are characterized by the value from VIP plot (Fig. 2C). The farther away from the origin, the higher the value of the ions in VIP score plot was.

The supervised PLS-DA analysis revealed a greater metabolic signature difference of the plasma from treated groups, compared to the control group (Fig. 2D). The R^2Y values and the Q^2 values of the PLS-DA model were 0.994, 0.899 in positive mode and 0.939, 0.936 in negative mode, indicating that the PLS-DA model was good to fitness and prediction. In PLS-DA score plot, licorice groups and kansui: licorice 1:4 group were close to the model group, while kansui group and kansui: licorice 4:1 group were close to the control group. The relative distances between treated groups (model, licorice 1, licorice 2, kansui, kansui: licorice 4:1, kansui: licorice 1:4) and the control group were calculated for quantization (Table 3). It can be obviously found that the order of relative distance in both modes is as follows: model group > kansui: licorice 1: 4 group > licorice 1 group > licorice 2 group > kansui group > kansui: licrice 4:1 group. It can be concluded that MPE model deviated the metabolite profiles from the normal states, demonstrating metabolism turbulence and significant pathobiological changes. The results showed that kansui group could regulate abnormal metabolism of MPE rats to the normal state, and kansui: licorice 4: 1 group had a better curative effect, while kansui: licorice 1: 4 group presented the opposite effect.

3.3. Metabolic profiling of heart, liver and kidney samples

The same procedures were employed for the metabolic profiling analysis of heart, liver, and kidney tissues. The PCA score plot of the control group and the model group showed that these two groups obtained good separation (Figs. 3A1, B1, C1). The potential biomarkers were extracted from the S-plot (Figs. 3A2, B2, C2) and VIP-value plot. Supervised PLS-DA (Figs. 3A3, B3, C3) were performed to explore the tendency of seven groups in both positive and negative modes. Furthermore, the relative distances between treated groups and the control group from PLS-DA score plot were calculated for quantization (Table 3). The same tread could be observed in heart, liver and kidney tissues. The results indicated that kansui group could adjust the abnormal metabolism of MPE rats to the normal state; kansui: licorice 4:1 group demonstrated better result while kansui: licorice 1:4 group showed worse result, and licorice 1 and 2 groups nearly had no impact on regulating the metabolism.

3.4. Identification and quantification of MPE biomarkers

According to the protocol detailed in metabolites identification, there were totally 57 differential metabolites contributing to MPE. Among the 19 metabolites identified in the plasma samples (Table S1), 11 metabolites were significantly increased, while 8 ones were significantly decreased in MPE model group compared to the

Table 2
Biochemical parameters of different groups.

Group	ALT (U/L)	AST (U/L)	ALP (U/L)	BUN (mmol/L)	CREA (μmol/L)	CK (U/L)
Control	35.2 ± 5.6	134.1 ± 16.3	86.6 ± 9.7	8.3 ± 0.8	57.7 ± 14.6	224.3 ± 37.4
Model	76.4 ± 7.3*	152.6 ± 18.5	97.6 ± 15.4	15.6 ± 2.1*	86.0 ± 9.2*	543.1 ± 63.2*
Kansui	48.5 ± 2.5#	145.0 ± 20.1	85.2 ± 18.5	9.5 ± 1.4#	42.8 ± 3.6#	380.3 ± 33.5#
Licorice 1	38.3 ± 5.3#	133.3 ± 24.6	93.2 ± 23.6	16.8 ± 1.7	78.1 ± 11.3	521.3 ± 54.3
Licorice 2	47.8 ± 10.9#	141.6 ± 17.0	87.3 ± 21.2	14.3 ± 2.5	88.7 ± 11.5	484.2 ± 46.4
Kansui:licorice4: 1	45.1 ± 8.2#	157.0 ± 26.4	94.0 ± 10.9	7.9 ± 0.9#	45.6 ± 4.5#	216.3 ± 51.8#
Kansui:licorice1: 4	64.7 ± 8.2	157.0 ± 26.4	104.3 ± 19.1	16.3 ± 1.5	87.7 ± 6.3	587.5 ± 46.8

* Compared with control group, $P < 0.05$.
# Compared with model group, $P < 0.05$.

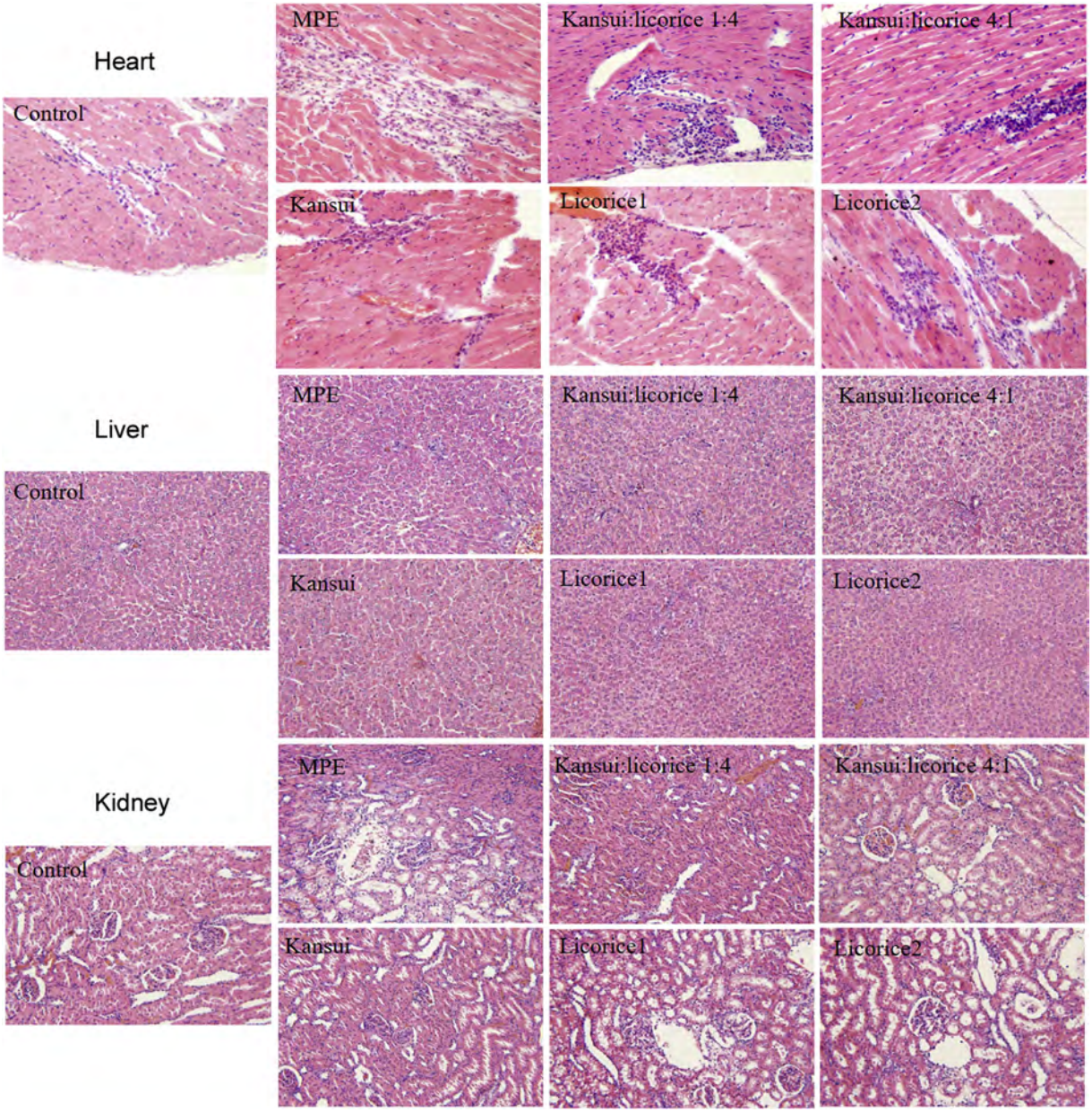

Fig. 1. Histological micrographs of heart, liver and kidney tissues stained with hematoxylin and eosin (original magnification 200 ×) in control group, MPE model group, kansui: licorice 1:4 group, kansui: licorice 4:1 group, kansui group, licorice 1 group, and licorice 2 group.

control group. The detailed information about metabolites in heart, liver and kidney samples is shown in Table S2, Table S3 and Table S4, respectively.

Additionally, to characterize the effects of kansui, licorice, and kansui-licorice combination, relative intensity of the differential metabolites in Tables S1–S4 were analyzed for semi-quantitation. It

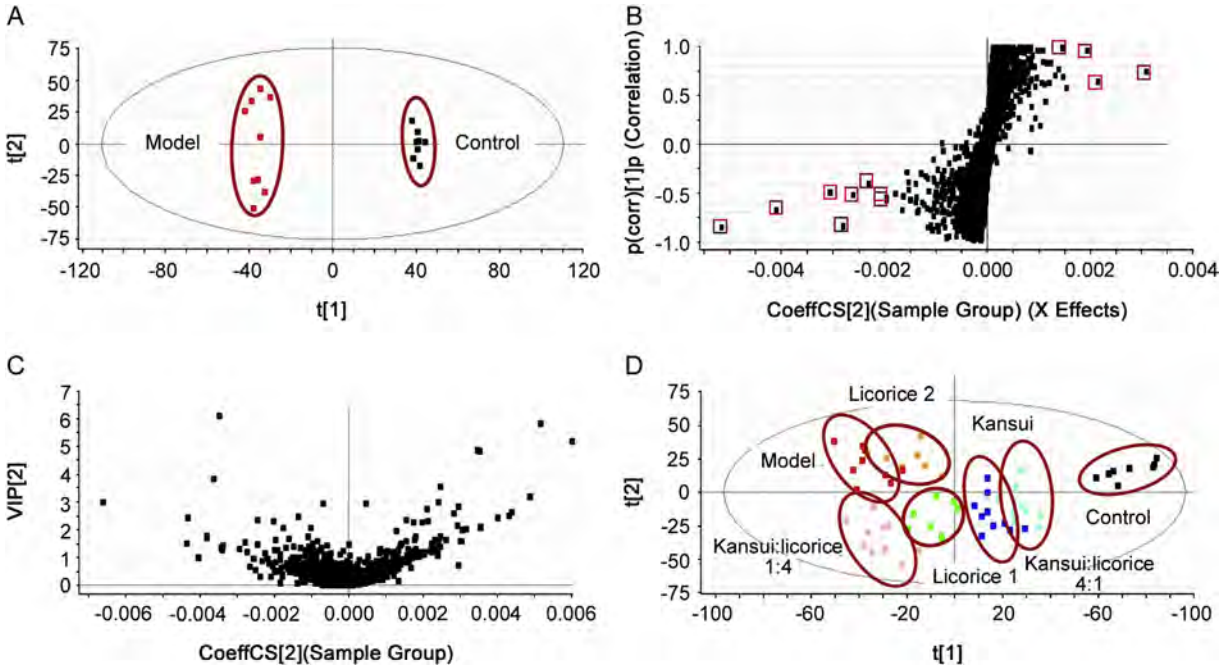

Fig. 2. The PCA score plot (A), S-plot (B), VIP-plot (C) of control and model groups, and the PLS-DA score plot (D) of all groups derived from plasma samples.

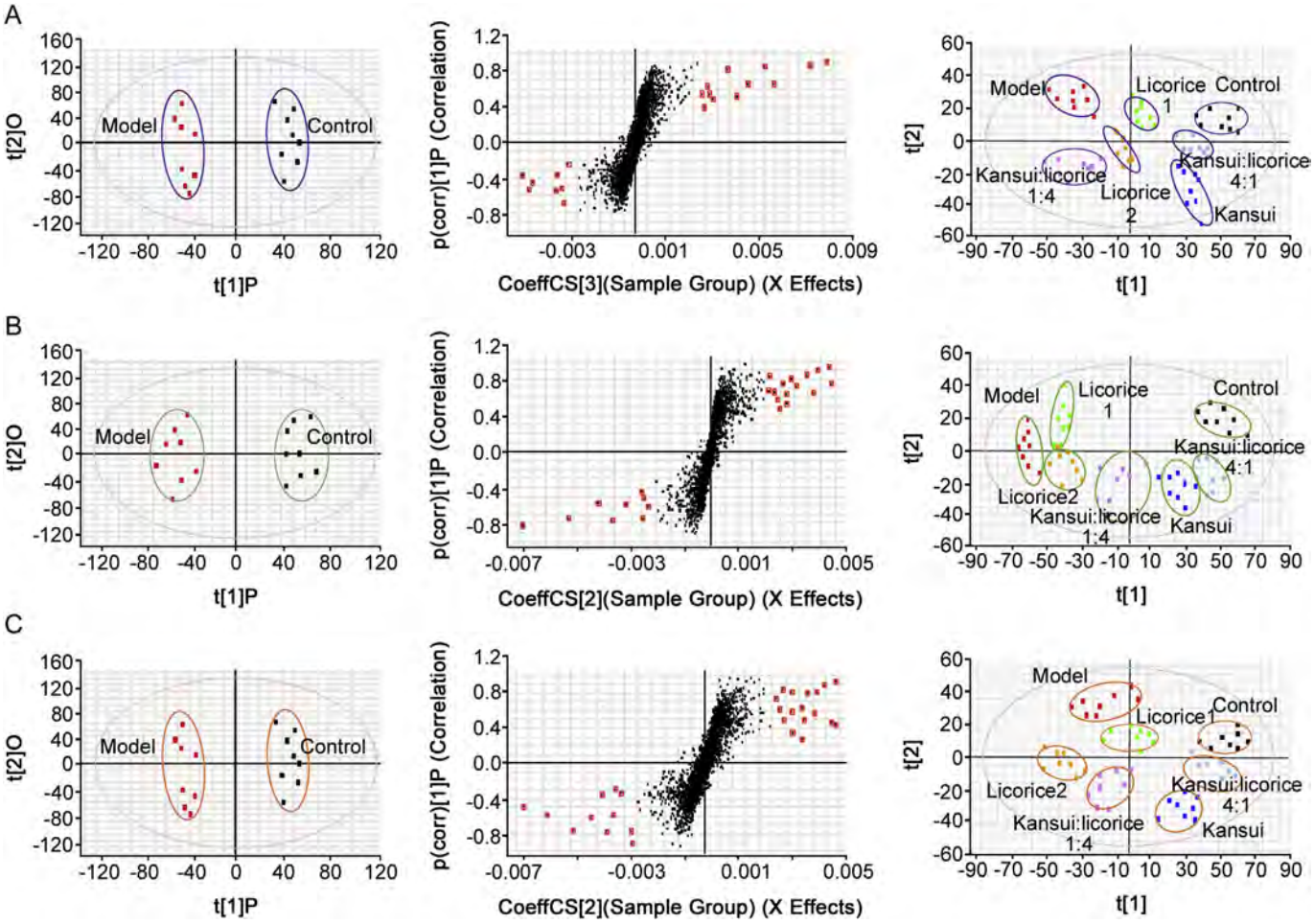

Fig. 3. The PCA score plot, S-plot and PLS-DA score plot derived from heart (A), liver (B), and kidney (C) samples.

Table 3
The relative distance between the treated groups and control group from the PLS-DA score plot of the plasma and tissue samples.

Sample	Mode	Control		Model	Kansui	Licorice 1	Licorice 2	Kansui:licorice 4 : 1	Kansui:licorice 1 : 4
		x-aix	y-aix						
Plasma	+	74.75	18.59	114.84 ± 7.96	68.08 ± 6.33*	98.79 ± 8.12	96.88 ± 8.02	32.05 ± 6.19*	118.52 ± 7.44
	−	57.41	−9.26	121.51 ± 6.22	54.14 ± 8.00*	110.17 ± 7.76	108.26 ± 6.66	43.10 ± 8.25*	115.34 ± 8.41
Heart	+	54.23	17.51	104.42 ± 6.85	57.12 ± 7.37*	83.20 ± 6.22	91.87 ± 7.41	25.40 ± 5.16*	98.34 ± 7.87
	−	43.61	−8.47	101.95 ± 7.27	49.41 ± 6.98*	89.62 ± 7.50	93.86 ± 8.19	34.25 ± 6.32*	95.56 ± 7.49
Liver	+	52.72	20.41	125.35 ± 7.26	65.28 ± 6.63*	108.75 ± 6.03	111.16 ± 8.37	43.36 ± 5.12*	89.22 ± 6.54
	−	39.31	−4.27	119.59 ± 8.42	58.15 ± 6.16*	102.86 ± 10.13	108.41 ± 8.25	50.17 ± 5.82*	83.25 ± 8.74
Kidney	+	59.36	21.42	123.35 ± 7.81	51.24 ± 7.45*	72.87 ± 6.89	105.76 ± 8.50	31.09 ± 5.73*	75.45 ± 7.68
	−	53.02	−8.47	112.57 ± 8.23	53.37 ± 7.83*	79.73 ± 7.65	99.53 ± 7.65	32.24 ± 6.45*	83.51 ± 6.81

*$P < 0.05$, compared with model group.

was found that compared to MPE group, 13 of 19 metabolites in plasma sample (Fig. S1), 11 of 15 metabolites in heart sample (Fig. S2), 14 of 18 metabolites in liver sample (Fig. S3), and 14 of 21 metabolites in kidney sample (Fig. S4) were adjusted to almost normal level in kunsui: licorice 4:1 group ($p < 0.05$). While the numbers of metabolites adjusted to normal level in plasma, heart, liver, and kidney sample were 2 of 19, 2 of 15, 2 of 18, and 0 of 21 by kunsui: licorice 1:4 treatment, and 13 of 19, 7 of 15, 8 of 18, and 11 of 21 by kansui treatment, respectively. The results indicated that kansui has a certain regulative action on MPE rats, and the effect can be enhanced by co-used with licorice at the ration of 4:1, but is weakened at the ration of 1: 4.

3.5. Calculation of biomarkers associated with compatibility and incompatibility

Heatmap was used to visualize the change trends of metabolites among groups and drawn by using Multi-experiment Viewer. To find out the biomarkers associated with compatibility and incompatibility in different rations of kansui-licorice combination, FC of kansui: licorice 4:1 group/model group or kansui: licorice 1:4 group/model group minus the corresponding single herb/model group is shown in Fig. 4. In the column of model/control, red represents up-regulation of metabolites by MPE, and in the column of (kansui: licorice 4:1 − kansui − licorice 1)/model, green represents the compatibility biomarkers leading to the synergism, while in the column of (kansui: licorice 1:4 − kansui − licorice 2)/model, red represents the incompatibility biomarkers leading to the antagonism. Similarly, in the column of model/control, green represents down-regulation of metabolites by MPE, and in the column of (kansui: licorice 4:1 − kansui − licorice 1)/model, red represents the compatibility biomarkers leading to the synergism, while in the column of (kansui: licorice 1:4 − kansui − licorice 2)/model, green represents the incompatibility biomarkers leading to the antagonism. Totally 29 compatibility biomarkers including 8 in plasma, 5 in the heart, 12 in the liver, and 6 in the kidney were identified, while 48 incompatibility biomarkers including 14 in the plasma, 12 in the heart, 16 in the liver, and 16 in kidney were identified.

3.6. Construction of metabolic pathways related to compatibility and incompatibility

To explore the metabolic pathways influenced by MPE and affected by kansui-licorice combination, endogenous metabolites identified above were imported into MetaboAnalyst and the pathways were constructed (Fig. 5). Arachidonic acid metabolism, sphingolipid metabolism, linoleic acid metabolism, glycerophospholipid metabolism, primary bile acid biosynthesis, pentose and glucuronate interconversions with -log(p) value>2 and impact value>0.1 were filtered out as the important metabolic pathways influenced by MPE. Five pathways including arachidonic acid metabolism, sphingolipid metabolism, linoleic acid metabolism, glycerophospholipid metabolism, synthesis and degradation of ketone bodies were regulated by kansui: licorice 4:1, which may indicate the compatibility mechanism. And 7 metabolic pathways including arachidonic acid metabolism, sphingolipid metabolism, linoleic acid metabolism, glycerophospholipid metabolism, synthesis and degradation of ketone bodies, pentose and glucuronate interconversions, butanoate metabolism were affected by kansui: licorice 1: 4, which may elucidate the incompatibility mechanism.

3.7. Statistical analysis identified key biomarkers and pathways of compatibility and incompatibility

The compatibility biomarkers in kansui: licorice 4:1 group and the incompatibility biomarkers in kansui: licorice 1:4 group are summarized in Table S5. The absolute values of the biomarkers obtained from the heatmap of normalized fold change (Fig. 4) were then analyzed. In the column of (kansui: licorice 4:1 − kansui − licorice 1)/model, blue represents the compatibility biomarkers leading to the synergism, and black represents the incompatibility biomarkers, while in the column of (kansui: licorice 1:4 − kansui − licorice 2)/model, orange represents the incompatibility biomarkers leading to the antagonism, and black represents the compatibility biomarkers (Table S5). The greater the value, the more important the biomarker is. For the common biomarkers of plasma and tissues, the value was summed by each tissue. Thus, biomarkers of glycocholic acid (1.89) in primary bile acid biosynthesis, prostaglandin F2a (1.54) in arachidonic acid metabolism, dihydroceramide (1.54) and sphinganine (1.51) in sphingolipid metabolism were filtered as the key biomarkers of compatibility. Biomarkers of sphinganine (2.73) and dihydroceramide (2.05) in sphingolipid metabolism, arachidonic acid (2.02) and leukotriene B4 (1.52) in arachidonic acid metabolism, acetoacetic acid (1.14) in synthesis and degradation of ketone bodies, and linoleic acid (1.05) in linoleic acid metabolism were filtered as the key biomarkers of incompatibility. The key biomarkers in metabolic pathways are shown in Fig. 6.

3.8. Expression of the pathway related cytokines and enzymes

Cytokines and enzymes were examined to further verify the influenced pathways. Three key pathways of arachidonic acid metabolism, sphingolipid metabolism, and primary bile acid biosynthesis identified above were used. Then related cytokines and enzymes in different groups were determined. The levels of sPLA2, AA, COX-2, PGF2α in serum were significantly decreased in kansui: licorice 4: 1 group while slightly changed in kansui: licorice

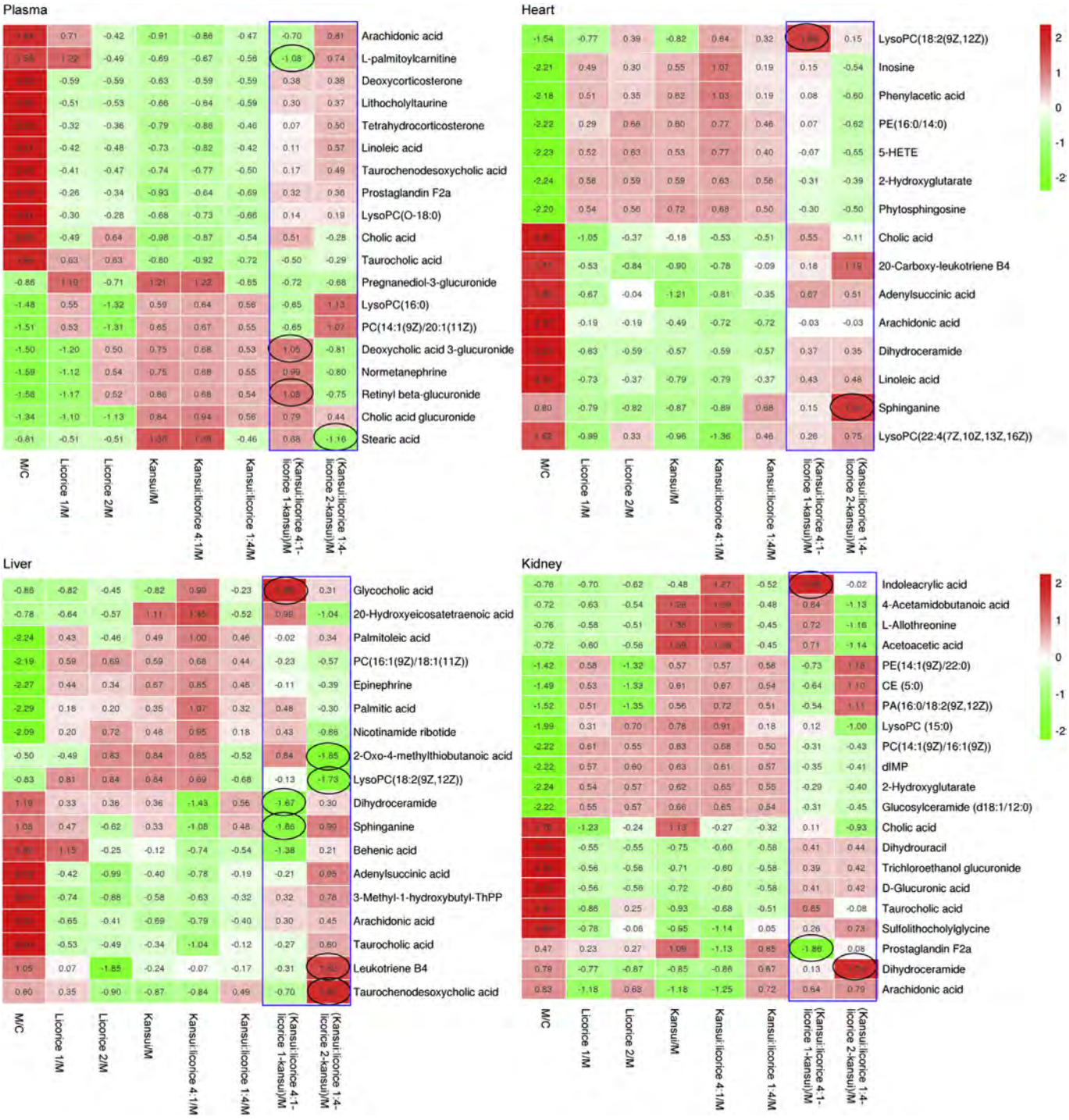

Fig. 4. Heatmap of fold change of metabolites screened out in plasma, heart, liver, and kidney.

1: 4 group compared with those in the MPE group. MPE caused a significant elevation in the level of SPT, and kansui: licorice 4: 1 group could markedly decrease the level. Meanwhile, serum concentrations of ACER1 and ACER2 were not influenced by MPE treatment, while that of ACER1 was significantly increased in kansui: licorice 1: 4 group. CYP7A1 and Tau were of great importance in primary bile acid biosynthesis; additionally, serum concentrations of them were increased in MPE group and kansui: licorice 1: 4 group compared with the control group, but was decreased in kansui: licorice 4: 1 group compared with MPE group (Fig. 7).

4. Disccusion

4.1. Metabolic feather of MPE affected by compatibility and incompatibility of kansui and licorice

Inflammation is an important progress of MPE. Arachidonic acid is the precursor for diverse inflammatory molecules. It can be synthesized by linoleic acid *in vivo*. Phospholipids from the plasma

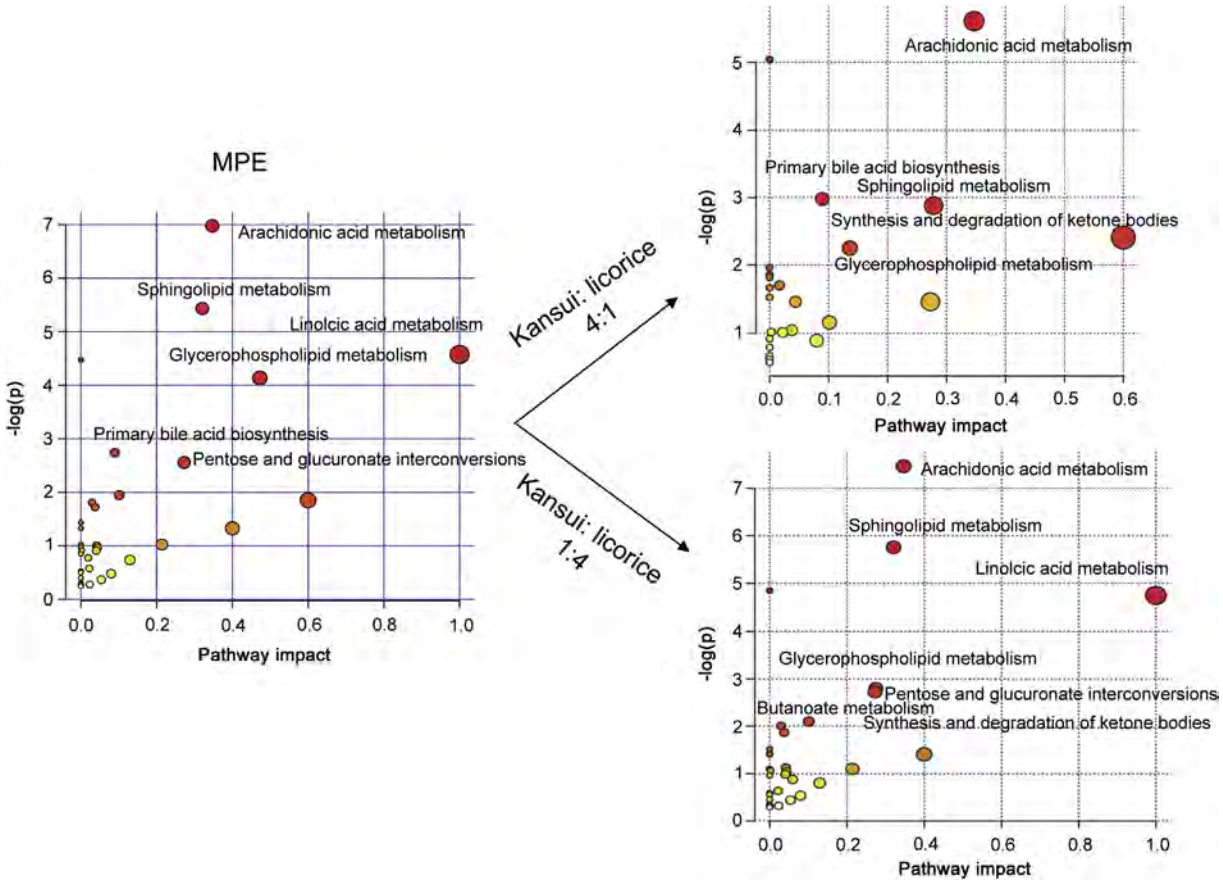

Fig. 5. Pathway analysis of MPE and affected by kansui: licorice 4:1 and 1:4 groups.

membrane are the primary source of arachidonic acid. A decreased level of PC was observed in the plasma, heart, liver and kidney tissues. However, the levels of partial LysoPC were greater in the plasma and tissues. PC could be converted into arachidonic acid by the enzyme catalysis of sPLA2. Although the level of PC was decreased, sPLA2 was upregulated, leading to the increase of the generation of endogenic inflammation molecules such as arachidonic acid. COX-2 can metabolize arachidonic acid to prostaglandin H2, which is subsequently processed by downstream enzymes to the various prostanoids [25]. In the present study, COX-2 was upregulated and the downstream product PGF2α was increased.

Sphingolipids constitute a class of lipids defined by their eighteen-carbon amino alcohol backbones synthesized from non-sphingolipid precursors. Modification of this basic structure gives rise to the vast family of sphingolipids that play significant roles in membrane biology and provide many bioactive metabolites in cell regulation as second messengers. Despite the diversity of structure and function of sphingolipids, their creation and destruction are governed by common synthetic and catabolic pathways. Sphingolipid metabolism can be imagined as an array of interconnected networks; additionally, sphingosine, phytosphingosine, and dihydrosphingosine are served as the backbones and ceramide is considered as the central molecule [26]. ACERs can catalyze the hydrolysis of ceramide to generate sphingosine, and sphingosine is further phosphorylated to produce sphingosine-1-phosphate. ACERs regulate the balance of ceramide, sphingosine and sphingosine-1-phosphate, and thus mediate cell proliferation, differentiation, survival, apoptosis, and tumor initiation and development. However, serum concentrations of ACER1 and ACER2 were not changed significantly in most of the groups except ACER1 in kansui: licorice 1: 4 group, suggesting that the turbulence of sphingolipid metabolism in MPE group has no concern with the two enzymes. Serine and palmityl-CoA can form 3- ketone -dihydrosphingosine under the catalysis of SPT, and then are converted to dihydrosphingosine and dihydroceramide, and finally form ceramide, and SPT is the speed limiting enzyme in the pathway. The levels of SPT are elevated significantly in MPE rats, which may cause the increase of sphinganine, dihydroceramide, and glucosylceramide in sphingolipid metabolism. Given that sphingolipids participate in most of the cellular processes, it is not surprising that sphingolipid metabolism is pivotal in the regulation of inflammatory signaling pathways [27].

Primary bile acid biosynthesis related to metabolites of cholic acid, taurocholic acid and taurochenodesoxycholic acid was observed to be upregulated in MPE rats. Thus, cholesterol 7α-hydroxylase (CYP7A1), the rate-limiting enzyme in the neutral pathway of bile acid biosynthesis [28], was determined. The result showed a significant increase of CYP7A1 in the control group and MPE group. The metabolism of cholesterol and bile acids is a primary function of normal liver cells, and the upregulated synthesis of bile acids may be associated with the hepatic injury. The metabolisms of cholesterol and bile acids by the gut microbiota have been known for decades. Cholesterol is mainly converted into coprostanol, a nonabsorbable sterol which is excreted in the feces. Primary bile acids (cholic and chenodeoxycholic acids) are converted to over twenty secondary bile acid metabolites by the gut microbiota. The main bile salt conversions include deconjugation,

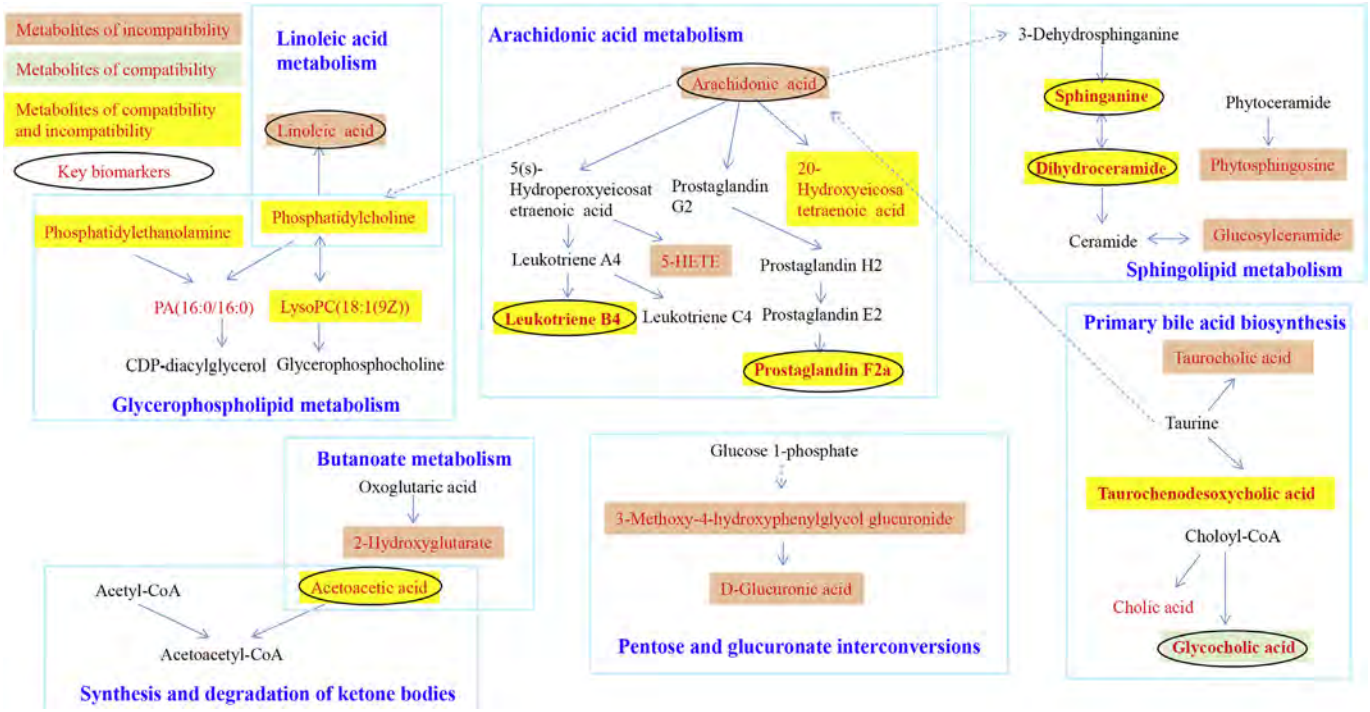

Fig. 6. Compatibility and incompatibility biomarkers in metabolic pathways.

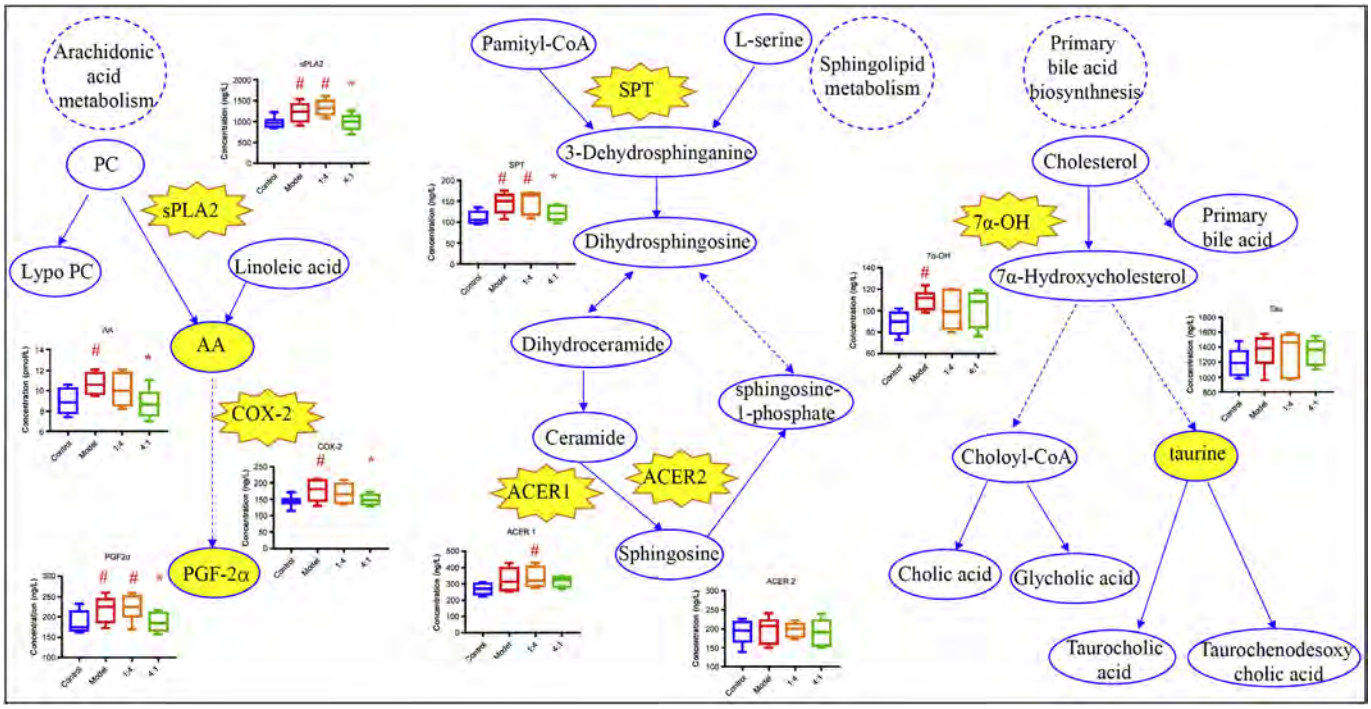

Fig. 7. Expression of the pathway related cytokines and enzymes.

oxidation and epimerization of hydroxyl groups at C3, C7 and C12, 7-dehydroxylation, esterification and desulfatation [29]. The significant increases in cholic acid, taurocholic acid and taurochenodesoxycholic acid suggest that the co-metabolism of gut microbiota is altered in MPE, and potential changes in the enterohepatic circulation may also have occurred.

4.2. An interactive heatmap to visualize complex metabolomics data and explore biomarkers of herb-herb interaction

Heatmap is one of the most widely used bioinformatics graphic displays [30]. It is especially popular in visualization of genomic data sets. Similar to genomic expression analysis, metabolomic experiment generates large data sets and heatmap is useful for

visual pattern recognition when searching for interesting features in the data, such as differentially expressed metabolites [31,32].

As is well known, multi-herb therapy is one of the most important characteristics of TCM, and herb-combination may lead to compatibility or incompatibility, but there are many obstacles in revealing the modernized connotation of multi-herb application due to the unimaginable complexity. The main reason is that herb-combination has a mixture of the characteristics of multi-components and multi-targets. Thus, it is difficult to accurately evaluate the efficacy or toxicity of TCM, which leads to the uncertainty and complexity of mechanism revealing. Metabonomic provides a valuable chance for understudying TCM with the similar characteristics of systematic and comprehensive [33], and exploratory data analysis including visual pattern recognition is developed for searching useful information.

The traditional heatmap provides a descriptive visualization of dysregulated metabolite features of single herb in each group, but it does not offer the opportunity to sort the data or reveal the biomarkers associated with herb-herb interaction. To overcome this limitation, we created an interactive heatmap with relative fold changes to display the underlying information. The relative fold changes of compatibility and incompatibility groups were calculated by relative abundance of ions of herb-combination minus single herb group. When comparing the dissimilarity heatmaps with fold changes for herb-combination group (Fig. 4, column 5–6) versus herb-combination minus single herb group (Fig. 4, column 7–8), there were stark changes in the two patterns. The changes caused by single herb were eliminated, and the biomarkers of compatibility and incompatibility screened out were more reliable. The results showed the potential and applicable of this data processing approach in deciphering the complex mechanisms of TCM compatibility and incompatibility. Thus, an interactive heatmap with relative fold change has been created to improve our ability to explore complex metabolomics data of herb-herb interaction. The interactive heatmap facilitates rapid recogniztion of biomarkers in herb-combination group, and also provides a novel means of viewing the metabolomic data to understand biological relationship of herb-herb interaction.

4.3. Untargeted tissue metabolomics revealed the target organs of compatibility and incompatibility of kansui and licorice

In this study, an untargeted plasma and tissue metabolomics approach was used to reveal the target organs of compatibility and incompatibility. As shown in Table S5, the values of plasma, heart, liver, and kidney were calculated by the absolute value of compatibility biomarkers minus the absolute value of incompatibility biomarkers, which were 2.85, −1.33, 9.72, and −0.27 in the column of (kansui: licorice 4:1 − kansui − licorice 1)/model, and −6.16, −7.93, −13.76, and −6.83 in the column of (kansui: licorice 1:4 − kansui − licorice 2)/model, respectively. It means that the liver (9.27) is the compatible target organ, while the heart (−13.76), liver (−7.93) and kidney (−6.83) are the incompatible target organs. The results are in accordance with the biochemical and histopathological indicators. The decreased level of ALT and the attenuated pathological changes of the liver in kansui:licorice 4:1 group reflected the synergistic effect. And more severe pathological injuries of the heart, liver, and kidney were observed in kansui: licorice 1:4 group, which means the antagonistic effect.

The tissue metabolome can more directly reflect metabolic deregulation than the body fluid metabolome, but the biomarkers for clinical diagnosis should return from the tissue to the biofluids. Venn diagram was used to show common metabolic differences in plasma and tissues between control and MPE rats. Plasma and tissues shared 6 common metabolites, which were arachidonic acid, prostaglandin F2a, linoleic acid, taurocholic acid, cholic acid, and taurochenodesoxy cholic acid (Fig. S5), and the levels of these metabolites were observed to be up-regulated significantly in MPE group in comparison with the control group ($p < 0.05$). Kansui: licorice 4:1 treatment decreased the level of these metabolites while kansui: licorice 1:4 treatment increased them or showed no influence on them.

As shown in the results, each tissue clearly has a metabolic profile; therefore, it is interesting to determine how reflective plasma is as a systemic readout of these different tissue profiles. Because of the relative ease and non-invasive nature of the collection protocols for most biofluids (plasma and urine), they are frequently employed as the sample material for investigation, although a possible drawback of biofluids is that they represent a systemic readout of a highly dynamic system rather than allowing tissue-specific readouts. For the metabolites studied in this method, plasma and tissues shared only 6 common metabolites. It is still rather unclear whether the serum profile reflects the physiology of the various tissues. It is generally believed that localized disease perturbations in the body are severe enough to spill over into the circulation, where they can be measured in a less invasive manner. This is also the fundamental principle in disease biomarker studies, where systemic circulating metabolites are sensitive and specific for a disease, acting as a biomarker.

Metabolomics applications in tissue, as a matrix for studying disease or intervention, come with several advantages, all of which derive from the fact that the target pathology/alterations are directly examined. Firstly, this allows for easier and more relevant mechanistic elucidation, which in turn can provide targets for intervention. Additionally, differentially produced metabolites can be more easily identified in the corresponding tissue, as they may be metabolized, excreted, diluted or confounded by the complexity of the biofluid after secretion by the tissue. After being identified as differentially produced within the tissue, subsequent follow-up using targeted methods with higher sensitivity may be applied in biofluids as a less invasive option.

4.4. Comparative metabolomics dissect the possible mechanism of compatibility and incompatibility of kansui and licorice

Kansui and licorice may exhibit synergistic or antagonistic effects in different combination design; however, the potential mechanism of this interesting phenomenon has not been well clarified. In this study, comparative metabolomics approach was used to dissect the compatibility and incompatibility mechanism of kansui and licorice on MPE rats. The abnormal metabolism of arachidonic acid, sphingolipids, and primary bile acid cause the cancer cells to modify the metabolic pathway to induce kinds of adverse consequences, such as inflammation and organ injury. Biochemical and histological analysis confirmed that the heart, liver and kidney were injured in MPE rats. These biochemical and pathological changes in tissues were obviously attenuated in kansui: licorice 4:1 group.

To further understand the metabolic connections of our detected metabolites in biologically important metabolic pathways, we performed a manual curation of metabolic pathways (Fig. 6) by searching these important metabolites from Figs. 4 and 5 in KEGG website. Overall, the changes of these important metabolites in kansui: licorice 1:4 group were quite different from those of in kansui: licorice 4:1 group. Most of the MPE disturbed metabolites were modified by kansui: licorice 4:1 treatment, for example, decrease of arachidonic acid, prostaglandin F2α and increase of 20-hydroxyeicosatetraenoic, 5-HETE in arachidonic acid metabolism, decrease of sphinganine, dihydroceramide in sphingolipid metabolism, and increase of taurocholic acid, and

taurochenodesoxycholic acid in primary bile acid biosynthesis were observed. What's more, the variation of pathway related to cytokines and enzymes of sPLA2, AA, COX-2, PGF2α, SPT and CYP7A1 was in accordance with the metabolites change, which confirmed that the damage was relieved in kansui: licorice 4:1 group compared with MPE group. However, 4 of the 6 MPE disturbed metabolite pathways were affected greatly and two new metabolite pathways were influenced by kansui: licorice 4:1, which may be the incompatibility mechanism. The regulation of different metabolic pathways may be one of the reasons for the compatibility and incompatibility of kansui and licorice.

5. Conclusion

The present study investigated metabolic variations in MPE rats and elucidated the possible compatibility and incompatibility mechanism of kansui and licorice by comparative metabolomics. Totally 57 metabolites were filtered and identified from plasma and tissue metabolome in MPE model, including 19 in plasma, 15 in the heart, 18 in the liver, and 21 in the kidney. An interactive heatmap with relative fold change was created to improve our ability to explore complex metabolomics data of herb-herb interaction. On the basis of relative contribution values on the heatmap of biomarkers, glycocholic acid, prostaglandin F2a, dihydroceramide and sphinganine were screened out as the principal alternative biomarkers of kansui: licorice 4:1 group, and sphinganine, dihydroceramide, arachidonic acid, leukotriene B4, acetoacetic acid and linoleic acid were screened out as those of kansui: licorice 1:4 group. And by calculating the values of biomarkers in each tissue, the liver was identified as the compatible target organ, while the heart, liver, and kidney were identified as the incompatible target organs. Furthermore, pathways of primary bile acid biosynthesis and sphingolipid metabolism were constructed as the most important pathways for compatibility, and arachidonic acid metabolism and sphingolipid metabolism were constructed as those for incompatibility. These results provided the evidence of compatibility and incompatibility of kansui-licorice and gave a better understanding of the compatibility property for the two herbs, which is helpful for rational utilization of herbs with certain toxicity in TCM clinic. The study was the first to reveal some innate important characteristics of herbs related to TCM "*Eighteen Incompatible Medicaments*" through comparative metabolomics approach, and also provided exploratory ideas and a method for studying and developing other incompatibility herbs. The interactive heatmap mode with "relative fold change" of biomarkers established here is useful for characterizing the compatibility and incompatibility relationship of kansui and licorice. This provides a new approach to mining the biomarkers and for further research on the mechanism of multi-drug application. Our study not only yields new insights into the investigation of TCM action but also provides the possibility of deciphering the complex mechanisms of herb-herb interaction.

Acknowledgments

This research was financially supported by the National Basic Research Program of China (2011CB505300, 2011CB505303), the National Natural Science Foundation of China (81603258, 81673599, 81773882), Key Research Project in Basic Science of Jiangsu College and University (14KJA360001), Youth Talent Project Funded by Shaanxi Higher Education Association for Science and Technology (20180307), and 333 High Level Talents Training Project Funded by Jiangsu Province (BRA2016387). This research was also financially supported by a project funded by the Priority Academic Program Development of Jiangsu Higher Education Institutions (PAPD) and the Discipline Innovation Team Program of Shaanxi University of Chinese Medicine (2019-YL10).

Conflicts of interest

The authors declare that there are no conflicts of interest.

Appendix A. Supplementary data

Supplementary data to this article can be found online at https://doi.org/10.1016/j.jpha.2019.05.005.

References

[1] Y.P. Tang, F. Chen, E.X. Shang, et al., Evolution and medicine-using analysis of eighteen incompatible medicaments in TCM, World Sci. Technol. 12 (2010) 593–599.
[2] S.P. Wang, Y.Y. Hu, W. Tan, et al., Compatibility art of traditional Chinese medicine: from the perspective of herb pairs, J. Ethnopharmacol. 143 (2012) 412–423.
[3] J. Shen, J. Kai, Y. Tang, et al., The chemical and biological properties of Euphorbia kansui, Am. J. Chin. Med. 44 (2016) 253–273.
[4] H. Ma, S.S. Yang, H. Lu, et al., Bioassay-guided separation of anti-tumor components from Euphorbia kansui by means of two-dimensional preparative high performance liquid chromatography and real-time cell analysis, Anal. Sci. 32 (2016) 581–586.
[5] T. Matsumoto, J.C. Cyong, H. Yamada, Stimulatory effects of ingenols from Euphorbia kansui on the expression of macrophage Fc receptor, Planta Med. 58 (1992) 255–258.
[6] L. Zhang, X.Y. Shu, A.W. Ding, et al., LC-DAD-ESI-MS-MS separation and chemical characterization of the inflammatory fraction of the roots of Euphorbia kansui, Chromatographia 70 (2009) 805–810.
[7] R. Yang, L.Q. Wang, B.C. Yuan, et al., The pharmacological activities of licorice, Planta Med. 81 (2015) 1654–1669.
[8] G. Pastorino, L. Cornara, S. Soares, et al., Liquorice (Glycyrrhiza glabra): a phytochemical and pharmacological review, Phytother Res. 32 (2018) 2323–2339.
[9] G.V. Obolentseva, V.I. Litvinenko, A.S. Ammosov, et al., Pharmacological and therapeutic properties of liquorice preparations (a review), Pharm. Chem. J. 33 (2012) 427–434.
[10] X. Wang, H. Zhang, L. Chen, et al., Liquorice, a unique "guide drug"of traditional Chinese medicine: a review of its role in drug interactions, J. Ethnopharmacol. 150 (2013) 781–790.
[11] X.H. Yang, X.H. Qiu, W.C. Zhang, Clinical effects of antagonistic herbs Radix glycyrrhizae-Euphorbia kansui in treating with cirrhosis ascites, N. J. Trad. Chin. Med. 37 (2005) 42–43.
[12] J. Guo, E. Shang, J. Zhao, et al., Data mining and frequency analysis for licorice as a "Two-Face" herb in Chinese Formulae based on Chinese Formulae Database, Phytomedicine 21 (2014) 1281–1286.
[13] W.Q. Huang, X.L. Cheng, H. Xiao, et al., Effect of licorice and kansui combination on the functions and pathological histomorphology of heart, liver and kidney in rat, Chin. J. Clin. Rehabil. 8 (2004) 5996–5997.
[14] A.H. Ding, Y.Q. Hua, J.A. Duan, et al., Effects of incompatible combination of Glycyrrhizae Radix et Rhizoma with Euphorbiae Pekinensis Radix, Kansui Radix or Genkwa Flos on rat ileal motility in vitro, J. Nanjing Univ. Trad. Chin. Med. 28 (2012) 345–349.
[15] J. Shen, J. Wang, E.X. Shang, et al., The dosage-toxicity-efficacy relationship of kansui and licorice in malignant pleural effusion rats based on factor analysis, J. Ethnopharmacol. 186 (2016) 251–256.
[16] J. Shen, Y.P. Tang, Y.C. Xu, et al., Dosage-toxicity-efficacy relationship of Kansui Radix in malignant pleural effusion models based on Walker 256 analysis, China J. Chin. Mater. Med. 41 (2016) 1713–1717.
[17] J.K. Nicholson, J.C. Lindon, E. Holmes, Metabonomics: understanding the metabolic responses of living systems to pathophysiological stimuli via multivariate statistical analysis of biological NMR spectroscopic data, Xenobiotica 29 (1999) 1181–1189.
[18] G.D. Wu, C. Compher, E.Z. Chen, et al., Comparative metabolomics in vegans and omnivores reveal constraints on diet-dependent gut microbiota metabolite production, Gut 65 (2016) 63–72.
[19] B. Diémé, S. Mavel, H. Blasco, et al., Metabolomics study of urine in autism spectrum disorders using a multiplatform analytical methodology, J. Proteome Res. 14 (2015) 5273–5283.
[20] J.L. Griffin, A.W. Nicholls, Metabolomics as a functional genomic tool for understanding lipid dysfunction in diabetes, obesity and related disorders, Pharmacogenomics 7 (2006) 1095–1107.
[21] Q. Huang, Y. Tan, P. Yin, et al., Metabolic characterization of hepatocellular carcinoma using nontargeted tissue metabolomics, Cancer Res. 73 (2013) 4992–5002.
[22] X. Wang, B. Yang, H. Sun, et al., Pattern recognition approaches and computational systems tools for ultra performance liquid chromatography-mass spectrometry-based comprehensive metabolomic profiling and pathways analysis of biological data sets, Anal. Chem. 84 (2012) 428–439.

[23] J. Xia, M.J. Benner, R.E. Hancock, NetworkAnalyst-integrative approaches for protein-protein interaction network analysis and visual exploration, Nucleic Acids Res. 42 (2014) W167–W173.
[24] J. Xia, D.S. Wishart, Using MetaboAnalyst 3.0 for comprehensive metabolomics data analysis, Curr. Prot. Bioinformat. 55 (2016) 1–9.
[25] T.G. Brock, R.W. Mcnish, M. Petersgolden, Arachidonic acid is preferentially metabolized by cyclooxygenase-2 to prostacyclin and prostaglandin E2, J. Biol. Chem. 274 (1999) 11660–11666.
[26] C.R. Gault, L.M. Obeid, Y.A. Hannun, An Overview of Sphingolipid Metabolism: from Synthesis to Breakdown, Springer, New York, 2010, pp. 104–107.
[27] G.H. Norris, C.N. Blesso, Dietary and endogenous sphingolipid metabolism in chronic inflammation, Nutrients 9 (2017) 1180–1203.
[28] S. Gupta, R.T. Stravitz, P. Dent, et al., Down-regulation of cholesterol 7alpha-hydroxylase (CYP7A1) gene expression by bile acids in primary rat hepatocytes is mediated by the c-Jun N-terminal kinase pathway, J. Biol. Chem. 276 (2001) 15816–15822.
[29] P. Gérard, Metabolism of cholesterol and bile acids by the gut microbiota, Pathogens 3 (2013) 14–24.
[30] L. Wilkinson, M. Friendly, The history of the cluster heat map, Am. Statistician 63 (2009) 179–184.
[31] P.H. Benton, J. Ivanisevic, D. Rinehart, et al., An interactive cluster heat map to visualize and explore multidimensional metabolomic data, Metabolomics 11 (2015) 1029–1034.
[32] H. Gowda, J. Ivanisevic, C.H. Johnson, et al., Interactive XCMS Online: simplifying advanced metabolomic data processing and subsequent statistical analyses, Anal. Chem. 86 (2014) 6931–6939.
[33] Y.M. Lao, J.G. Jiang, L. Yan, Application of metabonomic analytical techniques in the modernization and toxicology research of traditional Chinese medicine, Br. J. Pharmacol. 157 (2009) 1128–1141.